Graphene-Based Refractive Index Sensor Using Machine Learning for Detection of Mycobacterium Tuberculosis Bacteria

Juveriya Parmar, *Graduate Student Member, IEEE*, Shobhit K. Patel, *Senior Member*, *IEEE*, Vijay Katkar and Ayyanar Natesan

***Abstract*—Rapid detection of mycobacterium tuberculosis bacteria is very important in reducing tuberculosis disease. We propose a label-free graphene-based refractive index sensor using a machine learning approach that detects mycobacterium tuberculosis bacteria. The biosensor is designed for higher sensitivity by analyzing different parameters like substrate thickness, resonator thickness, and angle of incidence. Machine learning is applied to predict the values of absorption for different wavelengths. The machine learning model is applied to four different parameters (angle of incidence, substrate thickness, resonator thickness, graphene chemical potential) of the biosensor. The plus shape metasurface is placed above the graphene-SiO2 hybrid layer to improve the sensitivity. The comparative analysis with other published designs is also presented. The proposed sensor with its higher sensitivity and ability to detect mycobacterium tuberculosis bacteria can be used in biomedical devices for diagnostic applications. Experiments are performed to check the K-Nearest Neighbors (KNN)-regressor model's prediction efficiency for predicting absorption values of intermediate wavelengths. Different values of K and two test cases; R-50, U-50 are used to test the regressor models using the R^2 Score as an evaluation metric. It is observed from the experimental results that, high prediction efficiency can be achieved using lower values of K in the KNN-Regressor model.**

***Index Terms*—Sensor, Sensitivity, Machine Learning, KNN-Regressor, Tuberculosis**

I. INTRODUCTION

Tuberculosis (TB) is caused by mycobacterium tuberculosis bacteria. TB is a very serious and infectious disease and its detection is very important because early detection of TB helps cure it easily [1]. The late detection of TB results in the bad health condition of the patients [2].Identifying active tuberculosis (TB) is still a critical global health concern around the world.

J. Parmar was with electronics and communication department, Marwadi University, Rajkot. She is with Mechanical and Materials Engineering Department, University of Nebraska-Lincoln, USA. (Email:juveriyaparmar2@gmail.com)

S.K. Patel is with Computer Engineering Department, Electronics and Communication Department, Marwadi University, Rajkot. (Email:shobhitkumar.patel@marwadieducation.edu.in)

V. Katkar is with Computer Engineering Department, Marwadi University, Rajkot. (Email:vijay.katkar@marwadieducation.edu.in)

N. Ayyanar is with Department of Electronics and Communication Engineering, Thiagarajar College of Engineering, Madurai-620 015, Tamilnadu, India. (Email: naece@tce.edu).

(Corresponding author's: Ayyanar Natesan and Shobhit K. Patel)

The tuberculin skin test cannot tell the difference between latent and active tuberculosis. The limitations of interferon release tests are comparable. Sputum acid-fast bacilli staining has a substantial rate of false-negative results that is up to 50%. Nucleic acid amplification tests, such as GeneXpert MTB/RIF (Cepheid, Sunnyvale, CA, USA), are efficient, but they necessitate a robust infrastructure and the collection of a good quality sputum sample, which is typically unavailable in more than a third of HIV-infected people.A biosensor that detects TB at an early stage is very important.

The accurate detection of biosensors depends on their sensitivity and that's why higher sensitivity is essential in such biosensors [3]–[6]. High sensitivity biosensors are used insensing biomolecules like hemoglobin, urine, protein, glucose, etc[7,8]. There are two main types of biosensors: labeled biosensors and label-free biosensors. Label-free biosensors are widely used because of their higher sensitivity and selectivity compared to labeled biosensors.TB can be detected using a label-free electrochemical biosensor [9]. The traditional detection methods are not highly sensitive as compared to biosensors. Biosensors are used to detect mycobacterium tuberculosis with higher sensitivity[10] and TB with the help of antibodies [11]. Fiber optic-based plasmonic absorber is used to detect tuberculosis. The sensitivity can be increased with the use of metamaterials and graphene material. We introduced how graphene and metamaterials are useful in improving the sensitivity with a machine learning approach to predict the absorption. Further, refractive index (RI) based biosensors are highly explored for several utilizations and are remarkable among the commercial utilities of recent sensing applications. These sensing devices provide real-time results and affordable sample preparation. In these sensors, a change in RI of the region probed by the resonant mode causes a corresponding frequency shift of the optical resonance of the sensor. The change in resonant frequency is converted to the sensing signal.

Graphene is a unique material having excellent electrical and optical properties [12]. These unique properties of graphene can be used to increase the sensitivity of biosensors [13]. Graphene-based biosensors also help in detecting urea when the patient is on dialysis. Graphene oxide is a form of graphene which can be used in biosensors to detect cancer cells. Cancer cell detection in the early stage is very important as it reduces the causality rate [14]. A graphene-based biosensor with its higher sensitivity can be used for the detection of different biomolecules. C-shaped split ring resonator metasurface is used to increase the sensitivity [15]. Living bacteria are detected using graphene-based biosensors.

This article has been accepted for publication in a future issue of this journal, but has not been fully edited. Content may change prior to final publication. Citation information: DOI 10.1109/TNB.2022.3155264, IEEE Transactions on NanoBioscience

Bacteria detection improves medical diagnostics which helps in the early recovery of patients [16]. Patel et al. reviewed several graphene-based absorbers for biomolecule detection such as hemoglobin, urine, glucose, etc., and other applications [17].

Machine learning is a new trend that can be used in solving many photonics problems which also involved biosensing [18]. One of the important things in the biosensor is its sensitivity. This sensitivity can be increased by proper selection of different parameters of the design and the machine learning approach can help in designing it to improve the sensitivity. The activity analysis of them also can be carried out with machine learning [19] The machine learning method can be used to increase the identification of biomolecules in biosensor design. The remote monitoring of the covid-19 patient can also be done with machine learning [20].

The machine learning approach is the best fit to design biosensors with more accurate results. We propose a machine learning algorithm with a KNN-regressor model and applied it to three parameters namely substrate thickness, resonator thickness, graphene chemical potential, and angle of incidence. The absorption for these parameters is predicted with high accuracy using the KNN-regressor model. The paper is divided into four sections. The second section is based on biosensor design for TB detection. The third section is based on sensitivity analysis and the fourth section is based on machine learning prediction. The fifth section is presenting the concluding remarks about the proposed design and obtained results.

II. Design and Modeling

A graphene-based biosensor has been designed for mycobacterium tuberculosis bacteria detection. The Finite Element Method (FEM) is used for simulation which is carried out through the COMSOL Multiphysics simulator. The simulation is carried out using the periodic boundary conditions with the help of tetrahedral Delaunay tessellation meshing conditions with minimum element size of 5 nm using the wave optics module of COMSOL Multiphysics software.The design and its different geometrical parameters are analyzed using machine learning. The results are obtained in the form of absorption for different geometrical parameters, angle variation, graphene's chemical potential. The different values of the refractive index for different concentrations of biomolecules are taken. The range of these sample refractive indices are 1.343, 1.344, 1.345, 1.346, 1.347, 1.348, 1.349, 1.350, 1.351, 1.352 [21]. The graphene material is sandwiched between the resonator and substrate material as shown in Fig. 1. The resonator of plus shape metasurface is used. The material of this resonator is gold. The graphene monolayer sheet is sandwiched between resonator and substrate. The substrate is made up of silicon dioxide (SiO_2). In Fig 1, the 3D view of the design is presented in Fig. 1(a), the top view of the design is presented in Fig 1(b) and the front view is presented in Fig. 1(c) of the design. The substrate thickness is kept at 0.6 µm and the metasurface thickness is kept at 0.2 µm. The area of the proposed substrate structure is 25×22 µm^2. The width of the plus shape is kept at 2 µm.

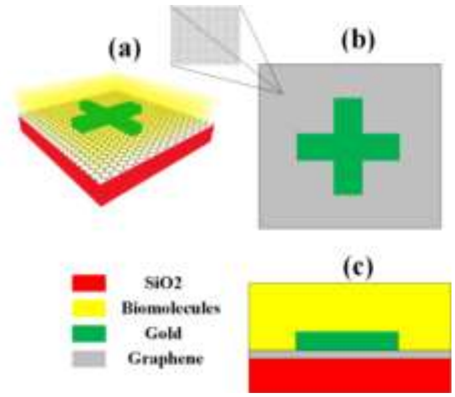

Fig. 1 Graphene-based plus metasurface biosensor design. (a) 3D view of the design (b) Top view of the design (c) Side view of the design. Graphene is sandwiched between gold metasurface and SiO_2 substrate. The substrate thickness is kept at 0.6 µm and the metasurface thickness is kept at 0.2 µm. The area of the proposed substrate structure is 25×22 µm^2. The width of the plus shape is kept at 2 µm.

a. *Sensitivity analysis:*

The sensitivity of any biosensor is dependent on two factors (a) change in wavelength (Δλ) and (b) change inrefractive index (Δn). It is inversely proportional to the refractive index change. The ratio of these two values gives the sensitivity as shown in Eq. (1) [22].

$$S = \frac{\Delta\lambda}{\Delta n} \tag{1}$$

b. *Graphene conductivity model and simulation:*

Graphene conductivity is very important which depends on its graphene chemical potential and it can be calculated using the Kubo formula [23]. The eq.are presented in Eq. (2-5). The intramodal (σ_{intra}) and intermodal (σ_{inter}) conductivity equations are presented in Eq. (2-5). ε_0 is the vacuum permittivity, σ_s is the graphene conductivity, ω is the angular frequency.

$$\varepsilon(\omega) = 1 + \frac{\sigma_s}{\varepsilon_0 \omega \Delta} \tag{2}$$

$$\sigma_{intra} = \frac{-je^2 k_B T}{\pi\hbar^2(\omega - j2\Gamma)}\left(\frac{\mu_c}{k_B T} + 2\,ln\left(e^{-\frac{\mu_c}{k_B T}} + 1\right)\right) \tag{3}$$

$$\sigma_{inter} = \frac{-je^2}{4\pi\hbar}\,ln\left(\frac{2|\mu_c| - (\omega - j2\Gamma)\hbar}{2|\mu_c| + (\omega - j2\Gamma)\hbar}\right) \tag{4}$$

$$\sigma_s = \sigma_{inter} + \sigma_{intra} \tag{5}$$

Parameter values of the eq. (2-5) have been shown in Table 1.

Table 1
Parameter values of graphene conductivity model

Parameters	Specification	Values
Δ	Graphene layer thickness	0.34 nm
Γ	Scattering rate	0.11 meV
ħ	Reduced plank constant	6.582119569×10^{-16}eV.s
k_B	Boltzmann constant	8.617333262145×10^{-5}e V.K^{-1}
μ_c	Graphene chemical potential	0.1 eV to 0.9 eV
τ^{-1}	electron relaxation time	10^{-13} s
T	Temperature	300K

This article has been accepted for publication in a future issue of this journal, but has not been fully edited. Content may change prior to final publication. Citation information: DOI 10.1109/TNB.2022.3155264, IEEE Transactions on NanoBioscience

III. Results and Analysis

The metasurface-based biosensor design and its details are presented in the previous section. In this section, the metasurface-based biosensor design is simulated using COMSOL Multiphysics with finite element method (FEM) and results are analyzed in the form of absorption. The design results by applying machine learning to find the best suitable parameters and highest sensitivity are also discussed in this section. The TB biomolecules are analyzed for different concentrations with their refractive index 1.343 to 1.352. The absorption results for these TB biomolecules are presented in Fig. 2. The wavelength shift for different concentrations is visible in the plot. The sensitivity is analyzed based on this wavelength peak shift and refractive index difference between the two TB biomolecules. The comparative table for the sensitivity for these 10 different concentrations is presented in Table 2. The maximum wavelength shift of 1 nm is achieved which leads to the highest sensitivity of 1000 nm/RIU.

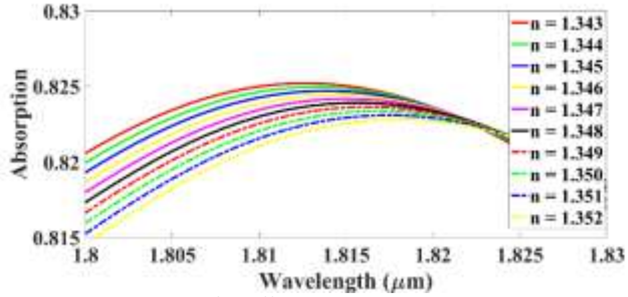

Fig. 2 Absorption results for different mycobacterium tuberculosis bacteria concentration samples with a refractive index ranging from 1.343 to 1.352.

TABLE 2
SENSITIVITY CALCULATION OF TB BIOMOLECULES WITH DIFFERENT CONCENTRATIONS AND THEIR REFRACTIVE INDEX RANGING FROM 1.343 TO 1.352

Parameters	TB biomolecules									
	n1	n2	n3	n4	n5	n6	n7	n8	n9	n10
n	1.343	1.344	1.345	1.346	1.347	1.348	1.349	1.350	1.351	1.352
Δn	0.001	0.001	0.001	0.001	0.001	0.001	0.001	0.001	0.001	
λ (μm)	1.813	1.8135	1.814	1.8145	1.815	1.816	1.8165	1.817	1.8175	1.818
Δλ (nm)	0.5	0.5	0.5	0.5	1	0.5	0.5	0.5	0.5	
S = Δλ/Δn	500	500	500	500	1000	500	500	500	500	

The design results are also analyzed for different variations of angle of incidence, substrate thickness, and resonator thickness, presented in Fig. (3-5). The substrate thickness is varied from 0.2 µm to 1 µm and its effect on absorption is observed in Fig. 3. The change in thickness of the substrate gives the increased path for absorption of energy which increases the absorption but an increase in substrate also changes the resonance so an increase in the thickness of substrate should be to a limit so that it does not affect the resonance wavelength. The change in angle is varied from 0º to 80º is shown in Fig. 4. Line plot and color plot are presented and results observed from 1.5 µm to 2.5 µm. In the line plot, results can be observed in the range of 2.1 µm to 2.5 µm. At angle 40º, a good response of absorption is achieved around 98% efficiency and the lowest absorption can be observed for 30º with 40% efficiency. In the color plot, the absorption efficiency result can be observed for the wavelength range of 1.9 µm to 2.2 µm, with angle variation 40º to 70º. So, we can say that the proposed refractive index sensor is wide-angle insensitive except for 30º as it achieved the lowest absorption for this angle. We can avoid this by placing a proposed sensor on a platform to avoid this angle of incidence and improved the quality of the proposed sensor.

The resonator thickness is also one of the key parameters in determining the resonance and absorption of the biosensor and it is presented in Fig. 5. It is simulated between 1.5 µm to 2.5 µm for separate values at 0.2 µm, 0.4 µm, 0.6 µm, 0.8 µm, and 1 µm. A good absorption efficiency around of 82% is observed at 0.8 µm followed by 1 µm around 78% efficiency. In the color plot, good results can be seen from 1.6 µm to 1.9 µm. It can be observed from the color bar given on the right side. We have not shown the graphene potential variation plot as there is not much absorption variation for different graphene chemical potential. It remains almost the same. Then, we have obtained R^2 value of 0.9938, from the linear fitting equation, which ensures the linear sensing performance and good reproducibility as shown Fig. 6.

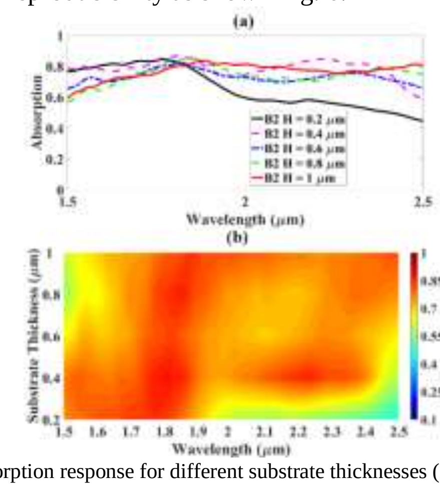

Fig. 3 Absorption response for different substrate thicknesses (B2H) ranging from 0.2 µm to 1 µm. (a) Line plot (b) Color plot. The wavelength range of observation is 1.5 µm to 2.5 µm. The negligible variation in absorption response by changing the substrate thickness.

We believe that the proposed sensor can be developed using the currently available fabrication techniques Molecular beam epitaxy (MBE) [24], Chemical vapor deposition (CVD) [25] and Cleavage [26] techniques are the basic methods of fabricating the two-dimensional and graphene-like single layer material. Graphene's top layer may be formed into the complex structure by using nano spheric lithography and nano-plasmonics lithography [27]. There are lithography methods for plasmonics device manufacturing that allow high quality graphene composites with complicated nano and microstructures, as shown in [27]. Graphene transfer printing with gold film may be used to transfer gold structure onto the graphene layer.

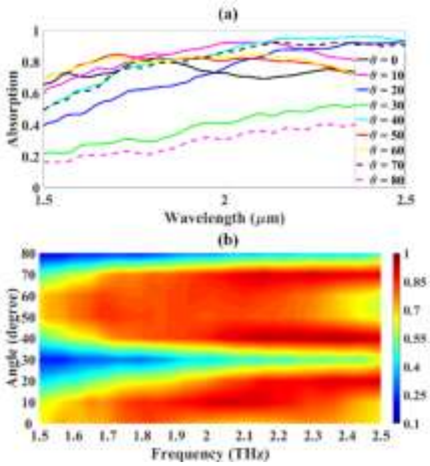

Fig. 4 Absorption response for Angle variation (degree) ranging from 0º to 80º. (a) Line plot (b) Color plot. The wavelength range of observation is 1.5 µm to 2.5 µm. Lower angle values are having better absorption.

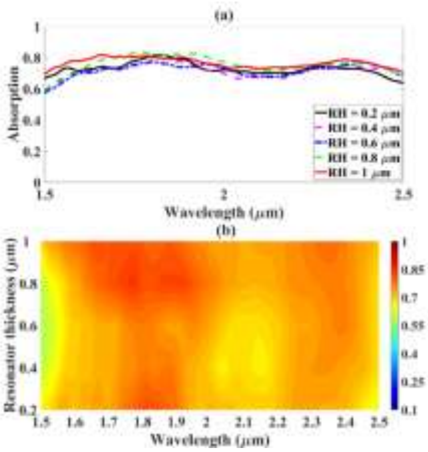

Fig. 5 Wavelength versus Resonator thickness (µm) plot. (a) Line plot (b) Color plot. The wavelength range of observation is 1.5 µm to 2.5 µm. The response is better for higher resonator thicknesses.

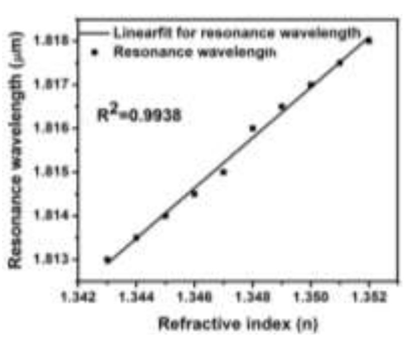

Fig. 6 Resonance wavelength change with varying refractive index of analyte

IV. Machine Learning Prediction using KNN-Regressor

Regression analysis is a statistical method for the detection of the relationship between dependent variable (Y) and independent variable (X) (eq. (6)).

$$Y = f(X) \tag{6}$$

In this research, absorption value is dependent variable and wavelength is independent variable. Due to non-linear relationship between absorption value and wavelength KNN-Regressor is used as a regression analysis model. KNN-Regressor accepts training dataset (D), number of neighbors to be used for regression analysis (K) and value of independent variable (I) as input to predict the value of independent variable (absorption in this case).

Input:

- Training Dataset 'D'
- Value of 'K'
- Value of Independent Variable 'I'

Procedure:

- Step 1: Calculate difference between 'I' and every value present in dataset 'D'
- Step 2: Select 'K' values from dataset 'D' with least difference from 'I'
- Step 3: SUM = Add target labels present in 'D' of 'K' number of closest values
- Step 4: Predicted Value = SUM / K

Euclidian distance is the most commonly used metric to measure the difference between 'I' and values present in dataset 'D'. Formula to calculate it is as follows(eq. (7)).:

$$difference(I, X) = \sqrt{\sum_{j=1}^{n} (I_j - X_j)^2} \tag{7}$$

Where n is number of attributes in training dataset

Performance of KNN-Regressor is measured using R^2 Score as a metric. It is calculated as follows (eq. (8-10)):

$$R^2 = 1 - \frac{SS_{red}}{SS_{tot}} \tag{8}$$

$$SS_{tot} = \sum_{i=1}^{M} (ActualTarget_i - \ Average\ TargetValue\ )^2 \tag{9}$$

$$SS_{res} = \sum_{1}^{M} (Predicted\ TargetValue_i - ActualTargetValue_i)^2 \tag{10}$$

Where SS_{res} is the sum of squares of the residual errors, SS_{tot} is the total sum of the errors and M is number of records.Experiments are performed using Python and scikit-learn library. The data obtained by the simulation process using COMSOL Multiphysics is used for experimentation. First-degree polynomial features are used to train the KNN-Regressor models. The KNN-Regressor is used to predict the absorption values of intermediate wavelength. Two test cases (R-50 and U-50) are used for testing the prediction efficiency of Regressor. 50 percent of randomly selected records from simulation data are removed and used to test the prediction efficiency in R-50. In U-50, Uniformly selected 50 percent records (even numbered records) from simulation data are removed and used to test the prediction efficiency.

This article has been accepted for publication in a future issue of this journal, but has not been fully edited. Content may change prior to final publication. Citation information: DOI 10.1109/TNB.2022.3155264, IEEE Transactions on NanoBioscience

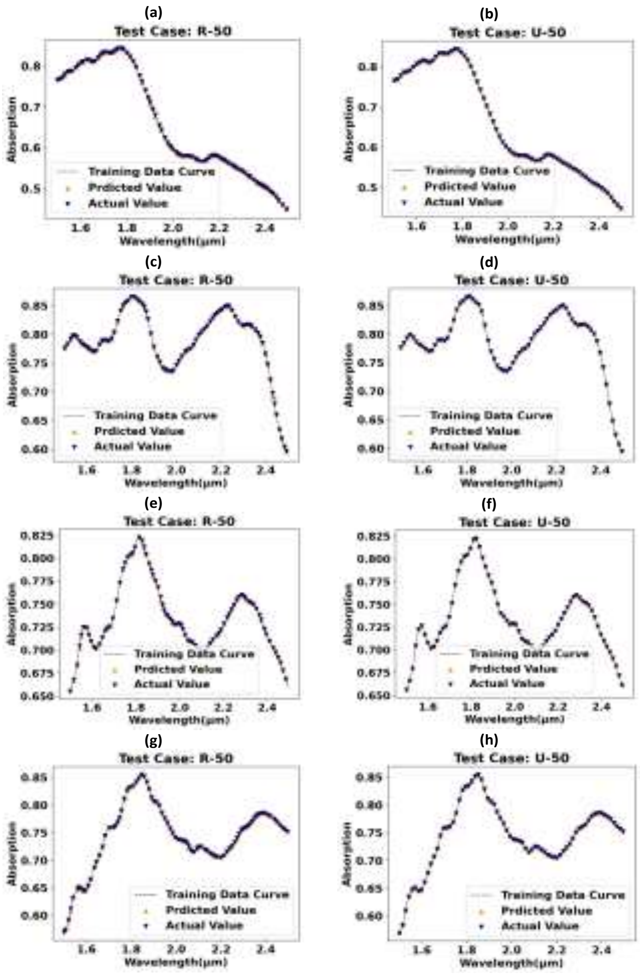

Fig. 7 Scatter Plot depicting the Actual and Predicted values of absorption for (a) Substrate Thickness 0.1 μm and K=2 (Test Case R-50) (b) Substrate Thickness 0.1 μm and K=2 (Test Case U-50) (c) Substrate Thickness 0.3 μm and K=2 (Test Case R-50) (d) Substrate Thickness 0.3 μm and K=2 (Test Case U-50) (e) Substrate Thickness 0.5 μm and K=2 (Test Case R-50) (f) Substrate Thickness 0.5 μm and K=2 (Test Case U-50) (g) Substrate Thickness 0.7 μm and K=2 (Test Case R-50) (h) Substrate Thickness 0.7 μm and K=2 (Test Case U-50)

Nonlinear relationship between absorption values and wavelength can be easily observed in Fig. 7. Fig. 7(a) and 7(b) shows the plot of actual absorption values with predicted absorption values for test case R-50 and U-50 respectively (Substrate Thickness = 0.1 μm). This figure proves that KNN-Regressor can predict absorption values of intermediate wavelength with high accuracy. Plots for substrate thickness 0.3 μm , 0.5 μm, 0.7 μm and two test cases (R-50, U-50) are shown in Fig 7(c)-7(d), 7(e)-7(f), 7(g)-7(h) respectively. Similar graphs can be created for angle of incidence, resonator thickness and graphene potential.

Prediction accuracy of KNN-Regressor for Assorted angles, graphene potential, resonator thickness, substrate thickness (Test Case R-50 & U-50) is shown in Fig. 8(a)-8(b), 8(c)-8(d), 8(e)-8(f), 8(g)-8(h) respectively. Fig. 8(a) shows that, highest prediction accuracy (R^2 Score) of 0.99966, 0.999876, 0.999977, 0.999942, 0.999964166, 0.999831738, 0.999878, 0.999956, 0.999928 is achieved for angle 0^0 (K=2), 10^0 (K=2), 20^0 (K=3), 30^0 (K=3), 40^0 (K=2), 50^0 (K=3), 60^0 (K=2), 70^0 (K=2) and 80^0 (K=2) respectively (Test Case R-50). As shown in Fig. 8(b), prediction accuracy (R^2 Score) of 1.0 is achieved for all angles (Test Case U-50).

As shown in Fig. 8(c), highest prediction accuracy (R^2 Score) of 0.99968, 0.99969, 0.99959, 0.99962, 0.99968 is achieved for graphene potential 0.1eV(K=3), 0.3eV(K=3), 0.5eV(K=3), 0.7eV(K=2) and 0.9eV(K=2) respectively (Test Case R-50). As shown in Fig. 8(d), highest prediction accuracy (R^2 Score) of 1, 0.99998, 1, 1, 1 is achieved for graphene potential 0.1eV(K=2), 0.3eV(K=2), 0.5eV(K=2), 0.7eV(K=2) and 0.9eV(K=2) respectively (Test Case U-50). As shown in Fig. 8(e), highest prediction accuracy (R^2 Score) of 0.99975, 0.99943, 0.999652, 0.99967, 0.99939 is achieved for resonator thickness 0.1μm(K=2), 0.3 μm(K=2), 0.5 μm(K=2), 0.7 μm(K=3) and 0.9 μm(K=4) respectively (Test Case R-50). As shown in Fig. 8(f), highest prediction accuracy (R^2 Score) of 1.0 is achieved for all values of resonator thickness (K=2 and Test Case U-50). As shown in Fig. 8(g), highest prediction accuracy (R^2 Score) of 0.99996, 0.99966, 0.99964, 0.99979, 0.99977 is achieved for substrate thickness 0.1μm(K=2), 0.3 μm(K=2), 0.5 μm(K=3), 0.7 μm(K=2) and 0.9 μm(K=2) respectively (Test Case R-50). As shown in Fig. 8(h), highest prediction accuracy (R^2 Score) of 1.0 is achieved for all values of substrate thickness (K=2 and Test Case U-50).

For K = 2, high absorption value prediction accuracy is achieved, indicating that absorption value for intermediate wavelength may be predicted with only two simulated data readings (i.e., reading of previous and next wavelength). To calculate the absorption value of intermediate wavelength, there is no need to include many previous and upcoming samples. As a result, simulation time and resource requirements in terms of computation time can be significantly decreased. In this case, it is approximately 50%, as KNN-Regressor can predict the absorption value of intermediate wavelengths with high accuracy. Even for K values 3 and 4, the KNN-Regressor predicts absorption values with high accuracy. However, it is not necessary to design a KNN-Regression model with a large K value because it can provide good prediction results for K value 2. We have also compared our design with other designs from references [28-36] to check the highest sensitivity. The comparison is presented in Table 3. It is evident that our design has the highest sensitivity compared to other designs.

TABLE 3.
COMPARATIVE TABLE OF SENSITIVITY

Biosensor Designs from References	Sensitivity (nm/RIU)
[28]	387.48
[29]	291.93
[30]	322.96
[31]	600
[22]	431.42
[32]	699.95
[33]	241.79
[34]	359
[35]	278.5
[36]	297
Proposed TB biosensor	1000

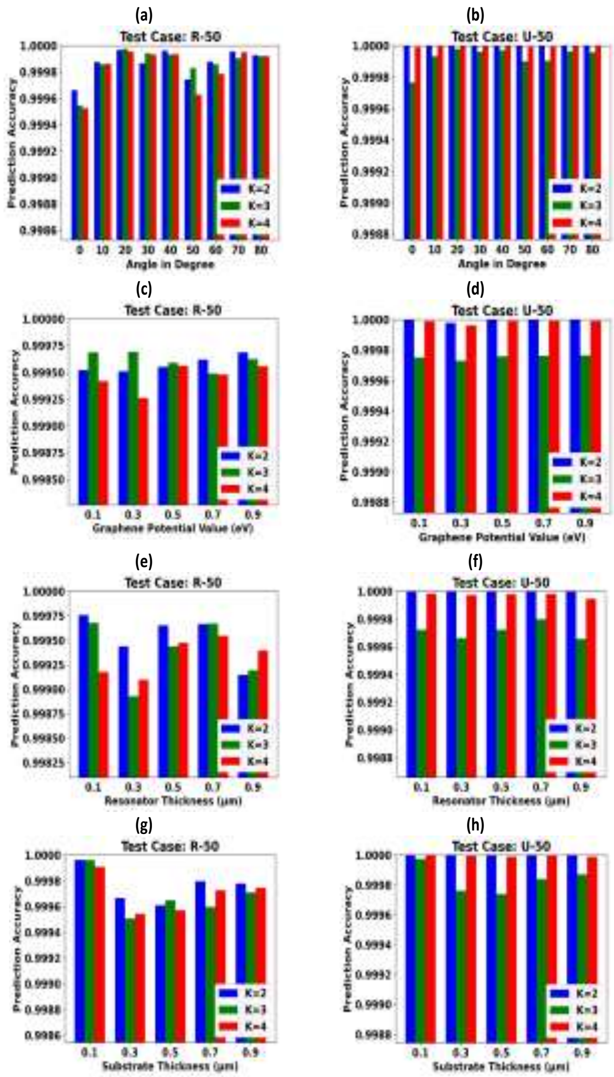

Fig. 8 Prediction Accuracy of KNN-Regressor for Assorted values of (a) Angle of Incidence & K (Test Case R-50) (b) Angle of Incidence & K (Test Case U-50) (c) Graphene Potential & K (Test Case R-50) (d) Graphene Potential & K (Test Case U-50) (e) Resonator Thickness & K (Test Case R-50) (f) Resonator Thickness & K (Test Case U-50) (g) Substrate Thickness & K (Test Case R-50) (h) Substrate Thickness & K (Test Case U-50)

V. CONCLUSION

We have presented a biosensor design for detecting mycobacterium tuberculosis bacteria. The biosensor is designed using a plus-shape metasurface based on graphene material. The novel machine learning approach is used for predicting the best values of different parameters such as graphene chemical potential, substrate thickness, resonator thickness, and angle of incidence. Graphene material used in the design gives a good impact on the sensitivity. Mycobacterium tuberculosis bacteria concentrations with different values of refractive index are analyzed and the highest sensitivity is achieved. The highest sensitivity is achieved 1000 nm/RIU. The sensitivity results are also compared with previously published results. Plus-shape metasurface made of gold used with graphene helps in increasing the absorption efficiency. Different geometrical parameters are varied for the biosensor metasurface design. The highest absorption efficiency of 82% is obtained around concentration having a refractive index of 1.34. The proposed biosensor with its high sensitivity and ability to detect mycobacterium tuberculosis bacteria can be applied to biomedical diagnostic applications. Experimental results prove that KNN-Regressor can be used as an effective tool for predicting absorption values of intermediate wavelengths. Experimental results also show that high prediction accuracy (more than 0.99 R^2 Score) is achieved using lower values of ‘K’.

REFERENCES

[1] J. Furin, H. Cox, and M. Pai, “Tuberculosis,” *The Lancet*. 2019, doi: 10.1016/S0140-6736(19)30308-3.

[2] A. Koch and V. Mizrahi, “Mycobacterium tuberculosis,” *Trends in Microbiology*. 2018, doi: 10.1016/j.tim.2018.02.012.

[3] C. Liu, D. Jiang, G. Xiang, L. Liu, F. Liu, and X. Pu, “An electrochemical DNA biosensor for the detection of Mycobacterium tuberculosis, based on signal amplification of graphene and a gold nanoparticle-polyaniline nanocomposite,” *Analyst*, 2014, doi: 10.1039/c4an00976b.

[4] K. Salimiyan Rizi *et al.*, “The overview and perspectives of biosensors and Mycobacterium tuberculosis: A systematic review,” *Journal of Cellular Physiology*. 2021, doi: 10.1002/jcp.30007.

[5] B. Golichenari *et al.*, “Electrochemical-based biosensors for detection of Mycobacterium tuberculosis and tuberculosis biomarkers,” *Critical Reviews in Biotechnology*. 2019, doi: 10.1080/07388551.2019.1668348.

[6] S. A. Taya, N. E. Al-Ashi, O. M. Ramahi, I. Colak, and I. S. Amiri, “Surface plasmon resonance-based optical sensor using a thin layer of plasma,” *J. Opt. Soc. Am. B*, vol. 38, no. 8, p. 2362, 2021, doi: 10.1364/josab.420129.

[7] Shobhit K. Patel ; Juveriya Parmar ; Rozalina Zakaria ; A Sharafali ; Truong Khang Nguyen ; Vigneswaran Dhaasarathan, “Sensitivity Analysis Of Metasurface Array-Based Refractive Index Biosensors,” *IEEE Sens. J.*, 2020, doi: 10.1109/JSEN.2020.3017938.

[8] S. K. Patel *et al.*, “Design of graphene metasurface based sensitive infrared biosensor,” *Sensors Actuators, A Phys.*, vol. 301, 2020, doi: 10.1016/j.sna.2019.111767.

[9] R. Nurmalasari, Yohan, S. Gaffar, and Y. W. Hartati, “Label-Free Electrochemical DNA Biosensor for the Detection of Mycobacterium Tuberculosis Using Gold Electrode Modified by Self-Assembled Monolayer of Thiol,” *Procedia Chem.*, 2015, doi: 10.1016/j.proche.2015.12.119.

[10] K. Chuensirikulchai *et al.*, “Sandwich antibody-based biosensor system for identification of Mycobacterium tuberculosis complex and nontuberculous mycobacteria,” *J. Immunoass. Immunochem.*, 2019, doi: 10.1080/15321819.2019.1659814.

[11] D. M, R. Bandaru, V. Janakiraman, and V. V. R. Sai, “A plasmonic fiberoptic absorbance biosensor for mannose-capped lipoarabinomannan based tuberculosis diagnosis,” *Biosens. Bioelectron.*, 2020, doi: 10.1016/j.bios.2020.112488.

[12] A. Geim, “Graphene — the perfect atomic lattice,” *Uspekhi Fiz. Nauk*, vol. 181, no. 12, p. 1283, 2011, doi: 10.3367/UFNr.0181.201112d.1283.

[13] N. F. Atta, A. Galal, and E. H. El-Ads, “Graphene — A Platform for Sensor and Biosensor Applications,” in *Biosensors - Micro and Nanoscale Applications*, 2015.

[14] S. A. Taya, I. Colak, B. Suthar, and O. M. Ramahi, “Cancer cell detector based on a slab waveguide of anisotropic, lossy, and dispersive left-handed material,” *Appl. Opt.*, vol. 60, no. 27, p. 8360, 2021, doi: 10.1364/ao.437738.

[15] S. K. Patel, J. Parmar, V. Sorathiya, R. Zakaria, V. Dhasarathan, and T. K. Nguyen, “Graphene-Based Plasmonic Absorber For Biosensing Applications Using Gold Split Ring Resonator Metasurfaces,” *J. Light. Technol.*, pp. 1–1, 2021, doi: 10.1109/JLT.2021.3069758.

[16] M. G. Daher, S. A. Taya, I. Colak, and O. M. Ramahi, “Design of a novel optical sensor for the detection of waterborne bacteria based on a photonic crystal with an ultra-high sensitivity,” *Opt. Quantum*

Electron., vol. 54, no. 2, p. 108, Feb. 2022, doi: 10.1007/s11082-021-03486-7.

[17] T. K. N. S. K. Patel, J. Surve, J. Parmar, "Review on Graphene-based Absorbers for Infrared to Ultraviolet Frequencies," *J. Adv. Eng. Comput.*, vol. 5, no. 4, pp. 214–238, 2021.

[18] F. Cui, Y. Yue, Y. Zhang, Z. Zhang, and H. S. Zhou, "Advancing Biosensors with Machine Learning," *ACS Sensors*. 2020, doi: 10.1021/acssensors.0c01424.

[19] "Activity Analysis Using Biosensor In Machine Learning," *Int. J. Pharm. Res.*, vol. 12, no. 04, 2020, doi: 10.31838/ijpr/2020.12.04.588.

[20] K. C. Un *et al.*, "Observational study on wearable biosensors and machine learning-based remote monitoring of COVID-19 patients," *Sci. Rep.*, vol. 11, no. 1, 2021, doi: 10.1038/s41598-021-82771-7.

[21] N. R. Ramanujam, S. K. Patel, N. Manohar Reddy, S. A. Taya, D. Vigneswaran, and M. S. Mani Rajan, "One-dimensional ring mirror-defect photonic crystal for detection of mycobacterium tuberculosis bacteria," *Optik (Stuttg).*, 2020, doi: 10.1016/j.ijleo.2020.165097.

[22] S. K. Patel *et al.*, "Graphene-Based Highly Sensitive Refractive Index Biosensors Using C-Shaped Metasurface," *IEEE Sens. J.*, 2020, doi: 10.1109/JSEN.2020.2976571.

[23] J. Surve, J. Parmar, S. K. Patel, and R. Jadeja, "Comparative analysis of metasurface array-based solar absorber for visible region," *Opt. Quantum Electron.*, vol. 53, no. 12, p. 696, Dec. 2021, doi: 10.1007/s11082-021-03355-3.

[24] E. Moreau *et al.*, "Graphene growth by molecular beam epitaxy on the carbon-face of SiC," *Appl. Phys. Lett.*, vol. 97, no. 24, p. 241907, Dec. 2010, doi: 10.1063/1.3526720.

[25] N. Petrone *et al.*, "Chemical Vapor Deposition-Derived Graphene with Electrical Performance of Exfoliated Graphene," *Nano Lett.*, vol. 12, no. 6, pp. 2751–2756, Jun. 2012, doi: 10.1021/nl204481s.

[26] K. S. Novoselov *et al.*, "Two-dimensional atomic crystals," *Proc. Natl. Acad. Sci.*, vol. 102, no. 30, pp. 10451–10453, Jul. 2005, doi: 10.1073/pnas.0502848102.

[27] T. Zou *et al.*, "High-speed femtosecond laser plasmonic lithography and reduction of graphene oxide for anisotropic photoresponse," *Light Sci. Appl.*, vol. 9, no. 1, 2020, doi: 10.1038/s41377-020-0311-2.

[28] S. Sahu, J. Ali, P. P. Yupapin, and G. Singh, "Porous Silicon Based Bragg-Grating Resonator for Refractive Index Biosensor," *Photonic Sensors*, 2018, doi: 10.1007/s13320-018-0459-z.

[29] X. Wang and C. K. Madsen, "Highly sensitive compact refractive index sensor based on phase-shifted sidewall Bragg gratings in slot waveguide," *Appl. Opt.*, 2014, doi: 10.1364/AO.53.000096.

[30] S. Sahu, J. Ali, P. P. Yupapin, and G. Singh, "Optical biosensor based on a cladding modulated grating waveguide," *Optik (Stuttg).*, 2018, doi: 10.1016/j.ijleo.2018.04.034.

[31] M. Sovizi and M. Aliannezhadi, "Design and simulation of high-sensitivity refractometric sensors based on defect modes in one-dimensional ternary dispersive photonic crystal," *J. Opt. Soc. Am. B*, 2019, doi: 10.1364/josab.36.003450.

[32] C. Teng *et al.*, "High-Sensitivity Refractive Index Sensor Based on a Cascaded Core-Offset and Macrobending Single-Mode Fiber Interferometer," *Front. Mater.*, 2021, doi: 10.3389/fmats.2020.595437.

[33] A. A. Badmos *et al.*, "High-sensitivity refractive index sensor based on large-angle tilted fiber grating with carbon nanotube deposition," in *Optical Sensing and Detection IV*, 2016, doi: 10.1117/12.2227703.

[34] H. Du, X. Sun, Y. Hu, X. Dong, and J. Zhou, "High Sensitive Refractive Index Sensor Based on Cladding Etched Photonic Crystal Fiber Mach-Zehnder Interferometer," *Photonic Sensors*, 2019, doi: 10.1007/s13320-019-0532-2.

[35] M. and M. Seifouri, "Numerical investigation of photonic crystal ring resonators coupled bus waveguide as a highly sensitive platform," *Photonics Nanostructures - Fundam. Appl.*, 2019, doi: 10.1016/j.photonics.2019.02.002.

[36] L. P. F. Peixoto, J. F. L. Santos, and G. F. S. Andrade, "Plasmonic nanobiosensor based on Au nanorods with improved sensitivity: A comparative study for two different configurations," *Anal. Chim. Acta*, 2019, doi: 10.1016/j.aca.2019.07.032.